Enhancing filtration knowledge to improve foundry performance

A Adams, Foseco Metallurgical Inc; O Davila-Maldonado, Instituto Politecnico Nacional, Mexico; L Oliviera, Foseco Industrial e Commercial ltda; and B Alquist, Foseco Morval Inc

While the ability of ceramic foam filters to reduce ductile iron inclusions has already been proven, a better understanding of filtration mechanisms will allow us to make better filters and enhance foundry performance.

The objective of the work was to define and quantify all the forces involved in molten metal filtration. In particular those that determine the trajectory of an inclusion and its likelihood of adhering to the filter matrix. This was achieved by developing a 3-D mathematical model based on physical water modelling and mathematical simulations. The laboratory experiments serve as a check against Foseco foundry experience and suggest avenues for enhanced filter design and application.

Introduction

Physical model

A plastic mould model (fig. 1) with a (1.0:1.1:3.0:1.4) gating ratio (S:R:F:G) was designed to test the reliability of the 3-D mathematical model described below. A controlled flow of water through the physical model was used to simulate iron flow. Polyamide seeding particles with neutral-buoyancy in controlled sizes (2-1000 microns) were added to the water to simulate slag inclusions.

A production ceramic foam filter was scanned and rapid prototype technology was employed to create a plastic foam filter for use in the physical mould model. The scanned dimensions and parameters were also used for the mathematical model.

An experimental system was constructed to represent iron flow and allow visual and physical measurements. The water model system centered on a runner system with a filter and utilised lasers, cameras, polyamide seeding particles, manometers and computers to measure and process various aspects of the fluid flow. The signals were sent to a PC where they were processed into dynamic pressure measurements, velocity, vorticity and streamline outputs (fig. 2).

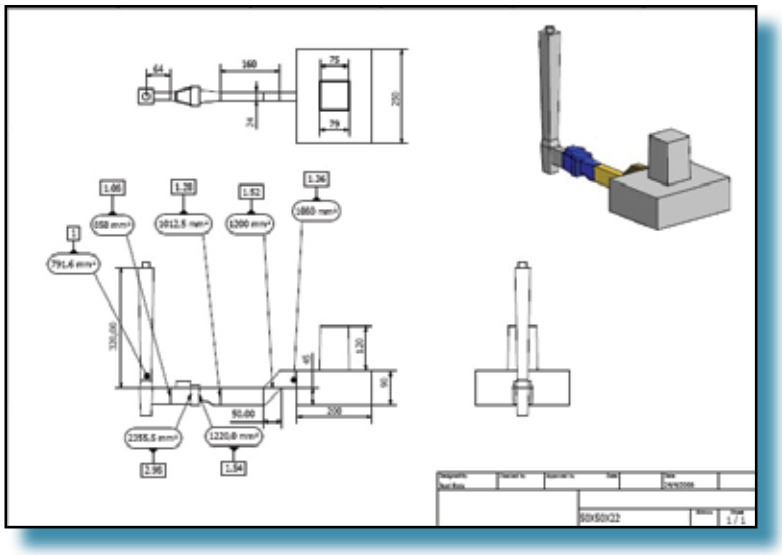

Fig. 1 Mould model

Mathematical Model

To mathematically simulate the trajectory of inclusions through the sprue, filter and runner, the following formula, based on Newton's second law relating to the acceleration of particles and the forces acting on them (drag, gravity, lift force), was used to determine the particle velocity:

$$mp\ dvp/dt = FD + FG + FL$$

Once the particle velocity is known, it is then possible to calculate its trajectory.

A number of assumptions regarding the temperature of the system, the shape of the particles, flow-direction coupling, particle surface and agglomeration were made to simplify the calculation.

Since casting flows are turbulent, a turbulence flow model must also be employed.

Detailed development of the mathematical model may be found in the technical paper upon which this presentation is based[1].

Computations were made for 2,570,000 cubic cells in the sprue, filter and runner for each iteration. To decrease computational load, the casting cavity was not included (fig. 3). During simulations, 1,000 inclusions of each size were

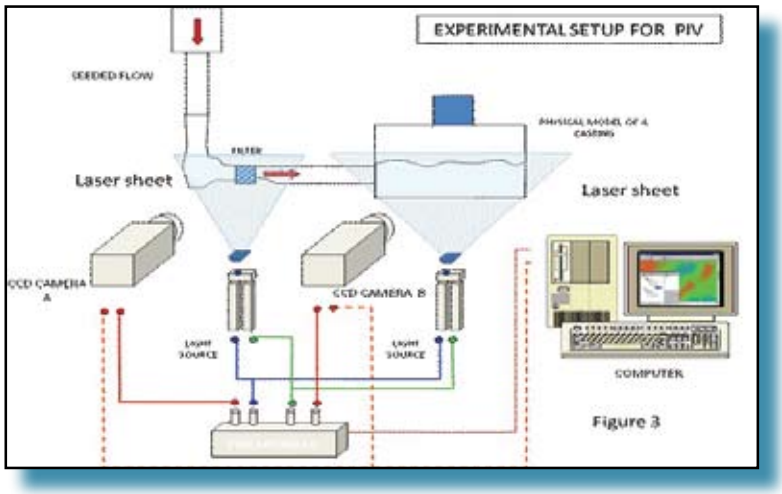

Fig. 2 Experimental setup

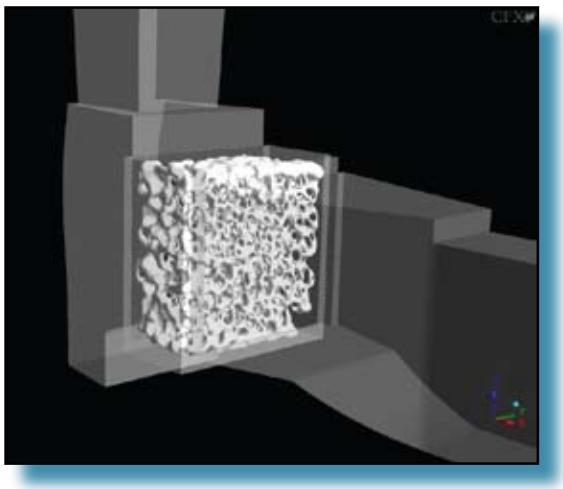

Fig. 3 Isometric view of the computational domain, including sprue, filter and runner

injected in the sprue. The trajectories of each particle were calculated and their statistical behaviour was used to characterise the different mechanisms involved during filtration of ductile iron melts.

Results and Discussion

Physical model

Fig.4a shows flow fields of water simulating a pouring rate of 292 kg/min of ductile iron in the plastic model without a filter. Fig.4b shows the same pouring rate with a filter.

The calculated flow fields are super-imposed over high-speed photographs taken of the physical model. The red colour corresponds to a maximum velocity of 0.80m/s and the dark blue, to velocities below 0.05m/s.

The model without the filter shows a melt stream with a very high velocity gradient that grows from the top to the bottom of the runner. This gradient is also seen at the midpoint of the runner and at its end. When a filter is used, there is a considerably decreased velocity gradient at the inlet. The stream has a plug flow pattern (nearly equivalent velocities across the runner) with smaller velocity gradients at the end of the runner.

The velocity gradient at the end of the runner greatly affects the amount of melt turbulence reaching the ingate and the casting. The flow without a filter will have higher velocities close to the runner bottom, and small velocities close to its top. This uneven profile will cause splashing and surface turbulence in the metal entering the casting cavity. The use of a foam filter reduces velocity gradients and the metal reaches the ingate and enters the casting with a more-symmetrical velocity profile and less turbulence.

Turbulence effects can also be visualised by introducing air bubbles into the liquid stream. The flow fields induced in a system without a filter and with a foam filter are shown in figs. 5a and 5b, respectively.

Without a filter, the uneven velocity gradient occurs and a significant number of large air bubbles are distributed throughout the stream. With a filter, there is a smaller velocity gradient and fewer, smaller bubbles are entrained by the stream. The filter resists the free passage of the two-phase flow, which loses its momentum. The bubbles decouple because the liquid decreases its velocity and they float toward the runner top.

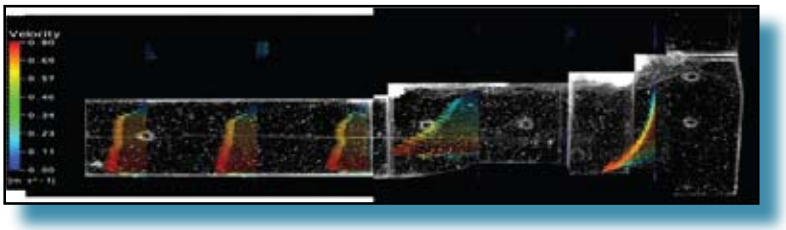

Fig. 4a Velocity fields inside the physical model without filter (flow right to left)

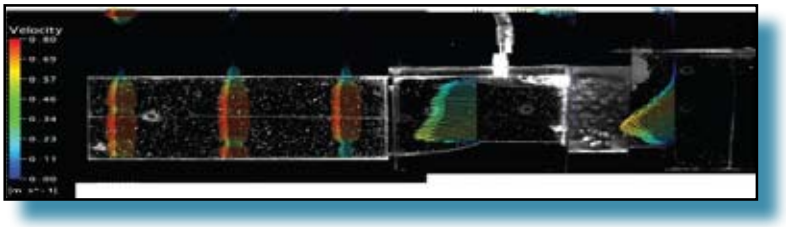

Fig. 4b Velocity fields inside the physical model with filter (flow right to left)

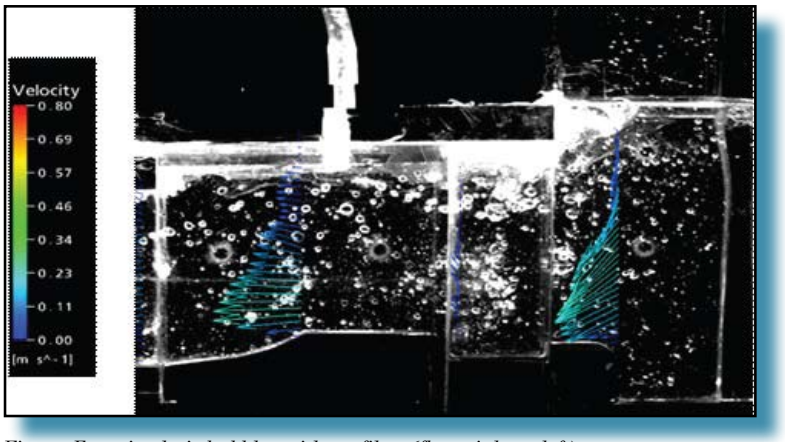

Fig. 5a Entrained air bubbles without filter (flow right to left)

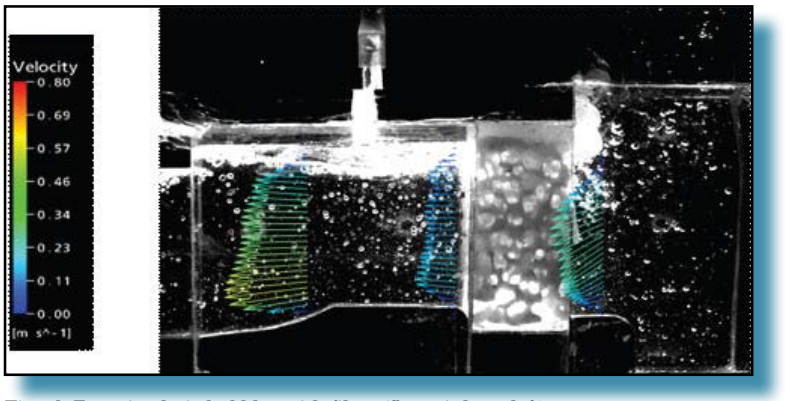

Fig. 5b Entrained air bubbles with filter (flow right to left)

Mathematical simulation

The reliability of the mathematical model was tested against results of the water model by comparing direct measurements of dynamic pressures obtained from the water experiments with the predictions of the 3-D simulations. The results are presented in figs 6a and 6b for cases without a filter and with a filter, at a pouring rate of 292 kg/min.

As can be seen, there is excellent agreement between numerical and experimental results without a filter and reasonable agreement for the results with the filter. The differences are small in terms of absolute pressure values, and it is reasonable to conclude that the mathematical simulations can reasonably predict physical results.

Filtration is a complex process, with multiple variables involved. These variables include the melt density, its viscosity, the diameter of the filter web, gravity, the inclusion size, its density, the turbulent diffusivity of the inclusions in the melt, and the superficial velocity of the melt through the cross section occupied by the filter.

Analysis shows that, among all variables influencing filtration of liquid metals, inclusion size is the most relevant. As the particle size increases, the response time of the particle becomes larger in relation to the dwell time of the melt inside the filter.

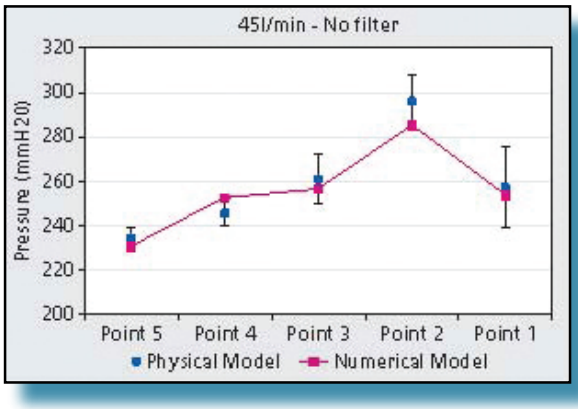

Fig. 6a Without filter

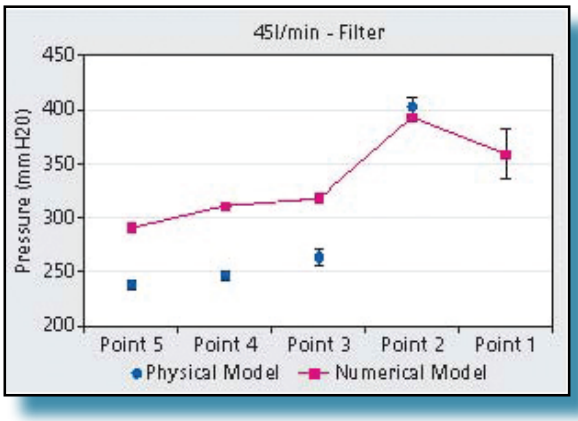

Fig. 6b With filter

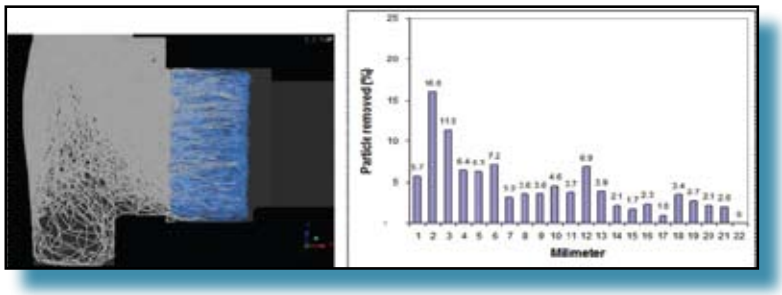

Fig. 7a Distribution of 2-micron particles captured along the filter thickness at a pouring rate of 292 kg/min

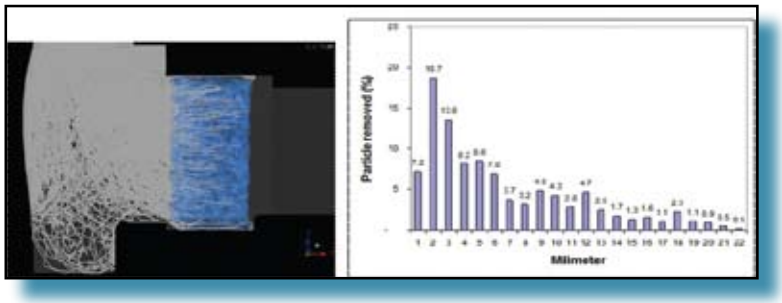

Fig. 7b Distribution of 100-micron particles captured along the filter thickness at a pouring rate of 292 kg/min

While pouring rate also has an influence, it is considerably less than particle size. This leads to the conclusion that particle size is the governing variable for filtration of ductile iron and will be the main parameter in the mathematical simulations below.

Figs. 7a and 7b show the mathematical simulations results for 2-micron and 100-micron inclusions, both at a pouring rate of 292 kg/min. The top image of each figure shows the trajectories in the central slice

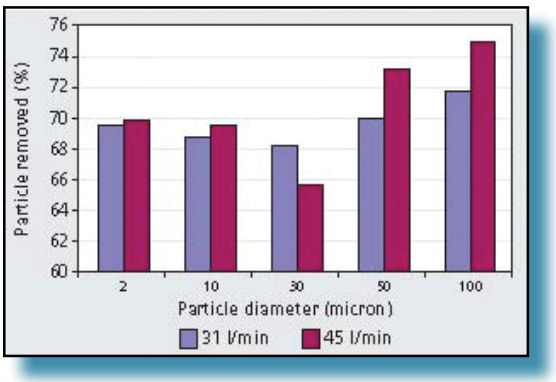

Fig. 8 Inclusions captured by impact-adhesion mechanism at different pouring rates

of the filter and the places where the inclusions are trapped in its interior. The bar plot shows distribution of inclusions trapped or captured along the thickness of the foam filter.

These results indicate that, for inclusions of 2 microns, about 85-90% of inclusions are captured in the first 15-16mm of filter thickness. For inclusions of 100 microns, 90% of inclusions are captured in the first 12mm of filter thickness.

As the inclusion size increases, it is expected that the capture region will be confined to the first 5mm of the filter thickness in cake and sieve filtration patterns. As the inclusion size decreases, one may expect a proportional increase in deep-bed filtration. These results can be summarised in fig. 8, where the percentages of inclusions trapped in the filter are plotted against the particle size for two different pouring rates.

As seen in fig. 8 small particle sizes are hardly affected by the pouring rate, indicating that inertia-drag forces are dominant over buoyancy forces.

As the inclusion size increases, one would expect that they would more easily penetrate the liquid film close to the matrix wall and adhere to it. Instead, the capture ratio decreases to a minimum seen at about 30 microns. This indicates that capture mechanisms other than simple impact-adhesion are at work.

Fig. 9 shows a close-up of the velocity fields present in a foam filter during flow rates of 45 l/min (the equivalent of 5.17kg in iron). Various types of micro-flows create a channeling effect. Some have high metal velocities, some have low, and others include both high and low velocity fields.

Hypothesis

With this wide spectrum of micro-flows, the trajectory of an inclusion is governed by a complex balance of all forces working on its volume and on its surface, i.e. buoyancy, adhesion, lift, drag and inertia.

A small particle flowing in the core of a high-velocity micro jet has limited capacity to penetrate the liquid film. Drag-inertial forces will dominate its trajectory and the metal will transport it through the filter.

A large inclusion in the same position, however, will be subjected more strongly to buoyancy and lift forces and, at some point, the inclusion may be

decoupled from the mainstream of the micro-jet and will float toward the web wall to adhere.

Where high and low melt velocities coexist, 'micro-free shear' flows form, with micro- boundary layers that include the transition from the high velocity micro-jet to the low velocity layer. If an inclusion makes contact with this boundary layer, lift and buoyancy forces exceed drag-inertial forces and the inclusion will be decoupled from the main stream regardless of its size. Once decoupled, its final destination will depend on its size. Large inclusions will float to the matrix wall and adhere. Small or medium inclusions will be trapped in the micro recirculating flow and remain there until the metal solidifies.

This hypothesis was tested using computer simulations of the trajectories of both large and small inclusions inside a foam filter under different pouring rates. The colours in the plots indicate the residence time of particles in seconds. The darkest red indicates residence times longer than five seconds.

With smaller inclusions (fig.10a), high pouring rates entrain and transport them to the outlet as indicated by the dark-blue lines corresponding to short residence times. Red spots indicate inclusions that have been decoupled from slow velocity fields and remain recirculating.

With medium and larger inclusions (fig.10b), as a result of the existence of free-shear micro-flows, many inclusions are trapped by recirculating flows. This leads us to the conclusion that they were decoupled from the micro-jets because lift and buoyancy forces exceed drag-inertial forces.

In total, these simulations confirm the original hypothesis regarding the relationships between inclusion size, inclusion capture and the various types of velocity fields within the liquid flow.

Conclusions

- The mathematical model developed in this work can be used to reliably predict pressure dynamic variations when measured using water modeling.
- A balance of buoyancy, drag and lift forces governs inclusion dynamics, with inclusion size as the variable with the most dominant influence on capture.
- Capture mechanisms as determined by this work include impact adhesion driven by direct contact, impact adhesion driven by flotation and decoupling from the main melt stream, and retention inside a filter pore of decoupled inclusion after pouring has stopped.
- Approximately 90% of inclusions of any size are captured in the first 15mm of a foam filter with a thickness of 22mm.
- Filtration patterns (cake, sieving and deep-bed) are heavily dependant on inclusion size.

The high degree of correlation between physical observations and calculated outcomes seen in this work justifies designing and conducting hot metal tests to confirm these results. This work will serve as the basis for improved filter design and application. It is part of the ongoing commitment of Foseco to improve foundry yield, scrap reduction, casting quality and productivity.

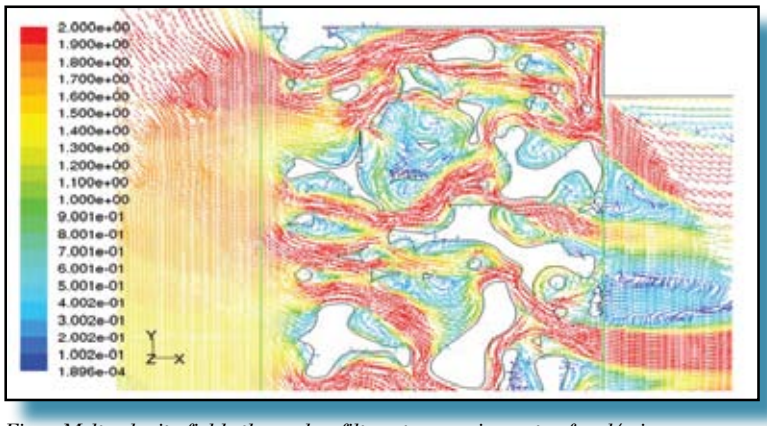

Fig. 9 Melt velocity fields through a filter at a pouring rate of 45 l/min

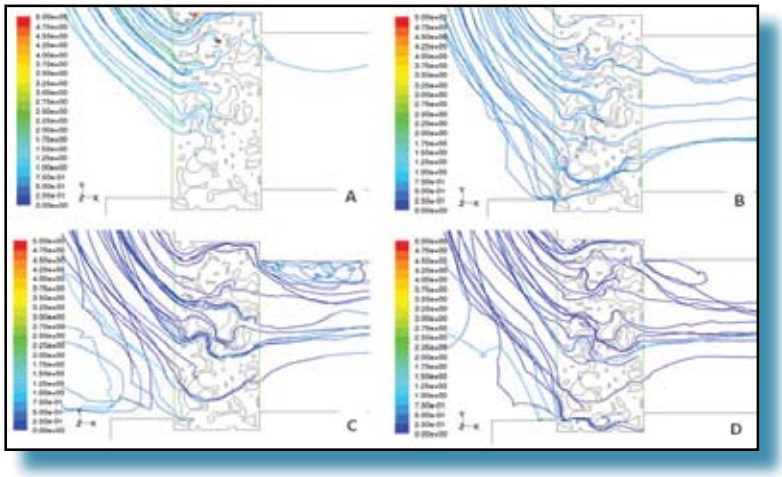

Fig. 10a Trajectories of small inclusions at various pouring rates. A 20 l/min, B 31 l/min, C 45 l/min, 12D 60 l/min

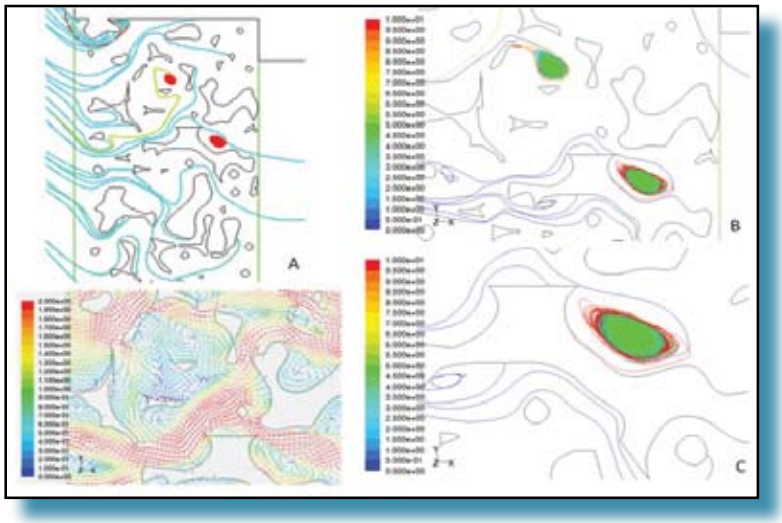

Fig. 10b Trajectories of medium and large inclusions at various pouring rates. A, 20 l/min for 2 microns, B & C 45 l/min for 200 microns

Reference

1. Morales R D, Davils-Maldonado O, Adams A, Oliviera L and Alquist B, *'Computer and fluid flow modeling of filtration mechanisms in foam filters'*. AFS Transactions, vol 116, pp715-731 (2008).

This paper was first published in Foundry Practice, published by Foseco, and is reproduced here with the publishers' kind permission.